A UNIQUE ELECTRIC DISCHARGE-EXCITED SOLID STATE X-RAY LASER

BY

ATANU RAFIQUE KHAN

THESIS

Submitted in partial fulfillment of the requirements
for the degree of Master of Science in Electrical and Computer Engineering
in the Graduate College of the
University of Illinois at Urbana-Champaign, 2012

Urbana, Illinois

Adviser:

Professor Emeritus George Miley

Abstract

A high-current discharge apparatus with a unique pulsed power supply was successfully constructed to demonstrate intense “anomalous” (exceeding direct charged-particle Bremsstrahlung) x-ray emission in the 1-2 keV range. Anomalous x-ray emission is attributed to ion implantation rather than normal electron Bremsstrahlung x-ray emission. A striking characteristic is that the x-ray energy can be several times the energy of the bombarding ions, suggesting a strong nonlinear mechanism. Such emission was observed during a glow discharge operation in the pressure range 0.1-5.0 torr with a cathode/anode separation of ~4.0 mm. This discharge operates at a voltage of 1-2 kV with a high-pulsed current up to 2 A. The current pulses have “square” time shape with 0.2-2.0 ms duration and a rise time of $0.1\ \mu s$.

Contents

1. Introduction

A. B. Karabut in the LUTCH Laboratory in Russia recently reported x-ray laser (approx. 1.5 keV) emission from metal targets such as Ti and Pd, which served as the cathode in a high-current pulsed Deuterium Glow Discharge (GD) plasma diode [1, 2]. Later, Karabut vividly demonstrated the potential capability of this type of laser with a 10 watt "prototype" unit, shown in Fig. 1. This prototype "drilled" a 9-mm diameter hole into a 3-cm thick plastic target (damage also extended out from the hole). This remarkable unit is more compact and provides a shorter wavelength than any prior "table top" x-ray laser.

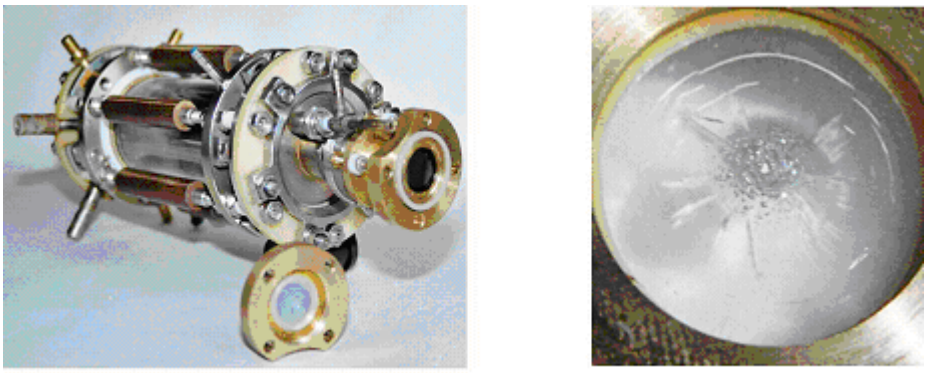

Figure 1: Photo of Karabut's prototype X-ray laser device (left) and photo detailing the accumulated damage to plastic target from laser operation (right). The damage pattern appears to be caused by many small beamlets rather than a solid beam.

The current project was initiated by staff at the University of Illinois Urbana-Champaign Campus (UIUC) to study the basic physics of this important new type of x-ray laser. Work in the first year of the project focused on both theoretical modeling and experimental studies. The UIUC experimental setup is based on Karabut's original design but has been upgraded to allow further in-depth scientific study. The UIUC is the first research group in the United States to take up research on this radical new type of laser [2, 3].

2. Experimental Setup

For operation of this high-pressure discharge, the UIUC team constructed a special pulsed power supply with the help of NMT. This unit was designed to duplicate the pulse waveform relative to rise and fall times reported by Karabut which is thought to be crucial for x-ray production. The unit however was designed to operate at higher power levels so that a broader parameter space could be studied. The unit is shown in Fig. 2.

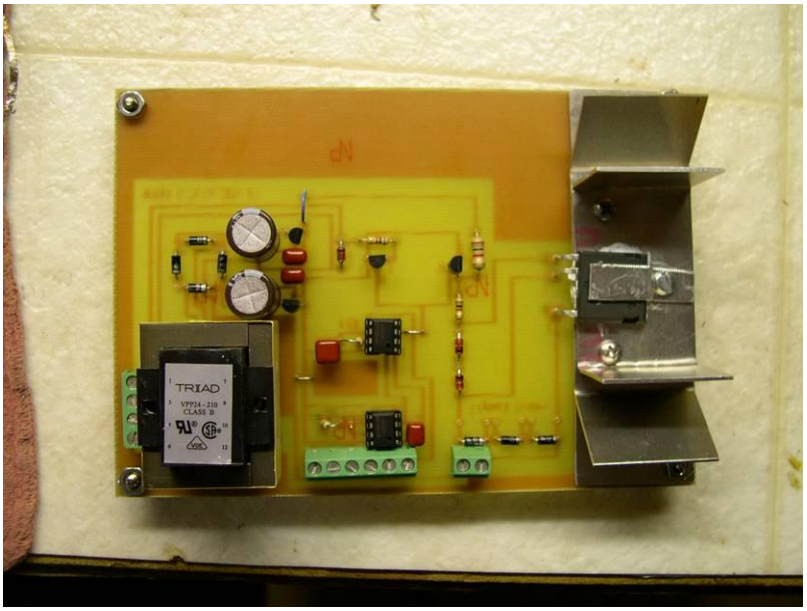

Figure 2: The 2.2-kVA power supply is shown. The circuit board controlling the frequency operates between 100 Hz and 1800 Hz and the pulse width modulation operates with duty cycles from 5% to 95%.

2.1. Basic Configuration

The vacuum chamber housing the UIUC discharge unit employed an existing spherical vacuum chamber shown in Fig. 3. The major components are described as follows:

- Water-cooling cathode (target can be mounted easily; capable of linear motion).
- Stainless steel anode (mounting device enables various angular states).
- K type thermocouple embedded between the target and the water-cooling jacket.
- Soft x-ray Detector.

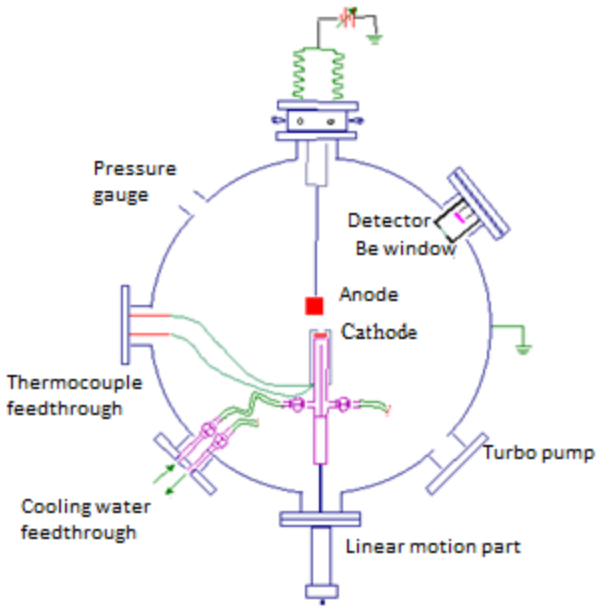

Figure 3: The large volume UIUC chamber gives room for internal diagnostics and thus the anode/cathode separation is easily adjusted.

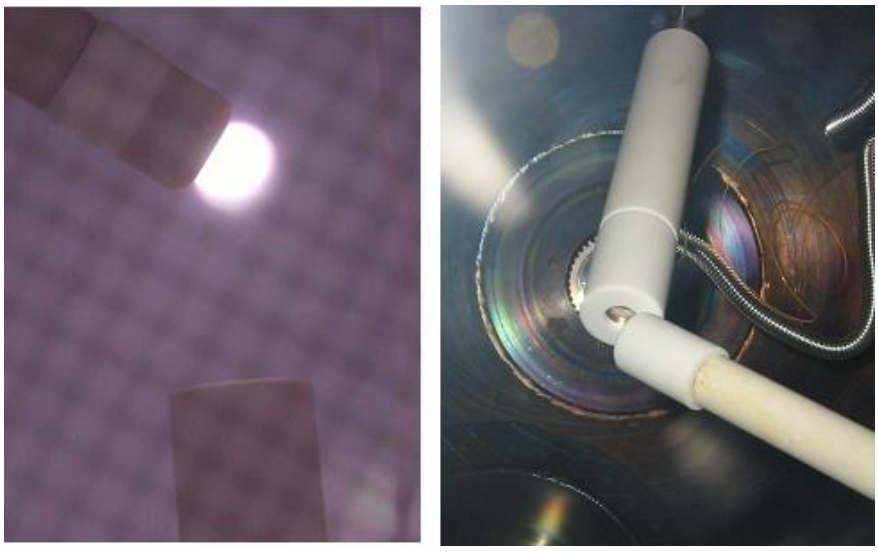

Figure 4: The Basic configuration is shown (left). A photo of the discharge is presented (right). The large volume UIUC chamber allows space for internal diagnostics.

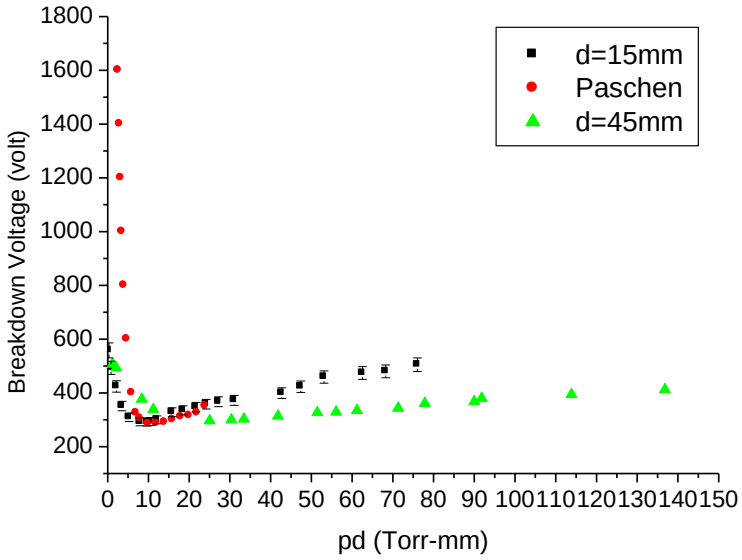

Figure 5: Ideal Paschen curve and the pd-V curve for basic configuration.

The basic configuration of Fig. 4 yields the pd-V curve in Fig. 5 which is termed as configuration 1. Results from experiments performed with a DC power supply to characterize the pd-V curve for this setup are shown in Fig. 5. It was determined that this configuration allowed excessive leakage of current which limited the discharge voltage. In configuration 1 the electrodes are at an angle of ~135°. The distances between electrodes ranged from 15 mm to 45 mm. To increase the applied voltage, five different electrode configurations were tested as described in the following sections.

2.2 Custom Configurations

2.2.1 Configuration 2

In configuration 2, the surface of the electrodes was parallel while the average distance between electrodes was markedly decreased compared to the basic configuration. The distance between the electrodes in Fig. 6 was 4 mm. To obtain better confinement of the discharge between electrodes, the macor shell was removed from the cathode, thus increasing the area of the cathode. The applied voltage-current curves, measured using DC power supply, are illustrated in Fig. 7. At pressures higher than 200 mtorr and currents higher than 20 mA, the discharge resides in the normal region. Namely, the voltage remains unchanged while the current increases until arcing occurs.

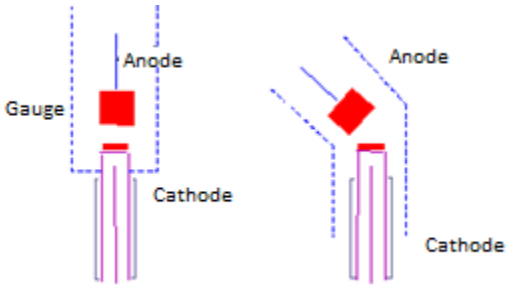

Figure 6: Configuration 3 showing an overhead (left), and an angular approach (right).

2.2.2 Configuration 3

The leakage current between the anode and the ground prevented the applied voltage from significantly increasing above ~0.5 kV in the first two configurations. Thus in configuration 3, the electrodes are surrounded by stainless steel gauze to reduce the leaking current. Here the gauze was grounded while in configuration 2, the gauze was left floating. The resulting steady-state I-V curves for various pressures are shown in Fig. 7. Comparing the resulting I-V curves with the basic configuration, we see that for the same pressure and current, configuration 3 can achieve a higher applied voltage.

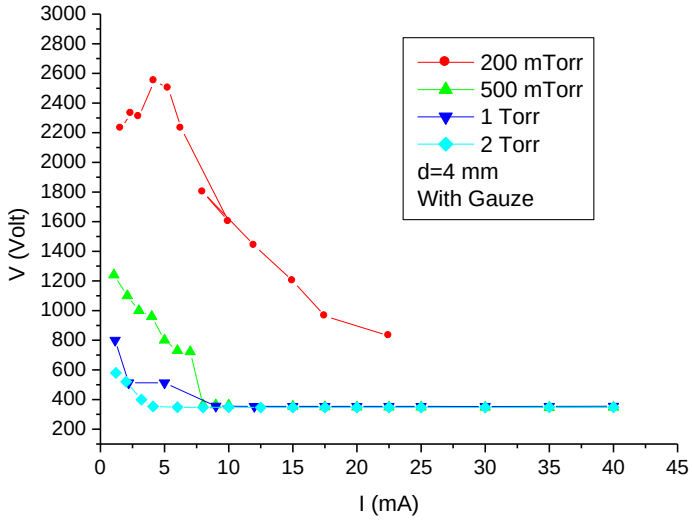

Figure 7: Steady-state applied voltage Pashcen curves for configuration 3.

2.2.3 Configuration 4

In an attempt to further reduce the leakage current and confine the plasma in a smaller volume, a glass tube was added to surround and isolate the electrodes (termed configuration 4). Plates covered by insulating material were used on both ends of the tube to provide a complete boundary for discharge. A hole of 1 cm diameter is drilled on one side of the tube to permit the passage of x-rays. A comparison of

the I-V curves for configuration 4 and configuration 2 is shown in Fig. 8. At 1000 mTorr the applied voltage in configuration 4 increased by nearly 50% compared to configuration 2.

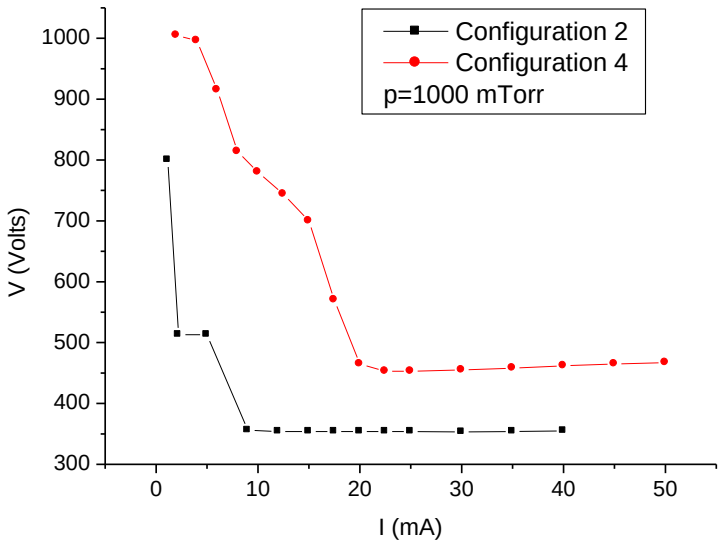

Figure 8: Comparisons of configuration 2 and 4.

2.2.4 Configuration 5

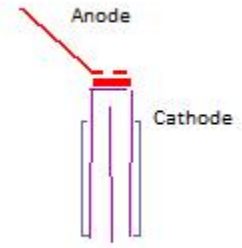

Figure 9: Configuration 5.

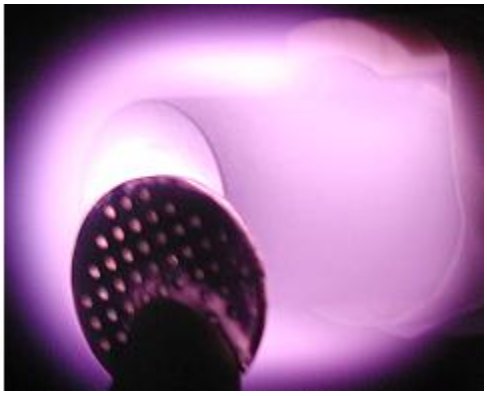

Figure 10: A photo of discharge for configuration 5.

One disadvantage of configuration 4 is that only the photons emitted by the electrode's surface at a select angel are collected by the detector. Thus in configuration 5 (Fig. 9), the anode is replaced by a stainless steel plate drilled with holes. In this configuration, the detector can be positioned so that the diode is directly facing the cathode. A photo of the discharge with the configuration 5 is shown in Fig. 10. However, it was confirmed that in this case, the applied voltage is very close to that in configuration 2. Hence this geometry does not offer a significant advantage compared to configurations 1-4.

Consequently this configuration was not employed in later x-ray experiments reported herein. However, it can be used later for certain diagnostic applications.

Based on these studies, configuration 4 was selected for subsequent studies based on its effectiveness for voltage holding and for ease of servicing the electrodes. Thus the following data was obtained with configuration 4.

2.3 Gas Mixture Effects

The effect of using a mixture of gases on discharge characteristics has also been investigated. The objective was to see if a higher discharge voltage could be achieved. In these tests, 10% of helium was added to the chamber at p = 500 mTorr and p = 1000 mTorr. However, Fig. 11 and Fig. 12 illustrate that the mixture of helium and deuterium did not effectively increase the applied voltage. As current goes to higher values, the mixture of gases will have the same applied voltage as the pure deuterium. Based on these results, only pure deuterium was employed in the x-ray experiments reported here.

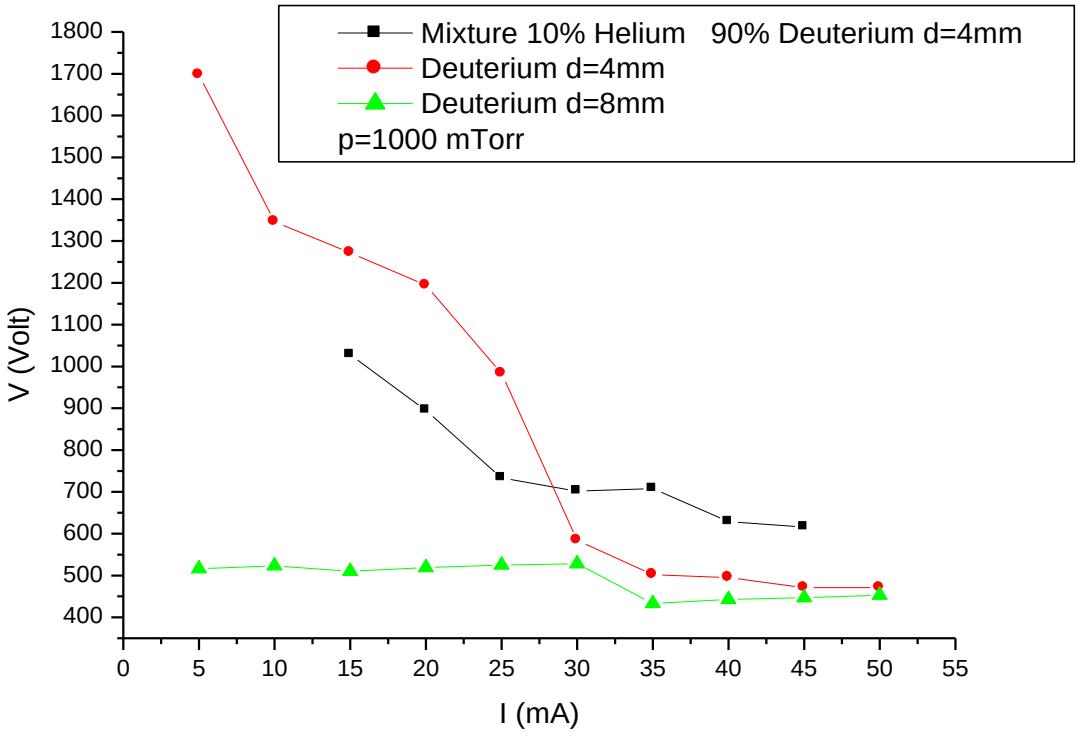

Figure 11: I-V curve for 10% of helium and 90% deuterium at p = 500 mTorr

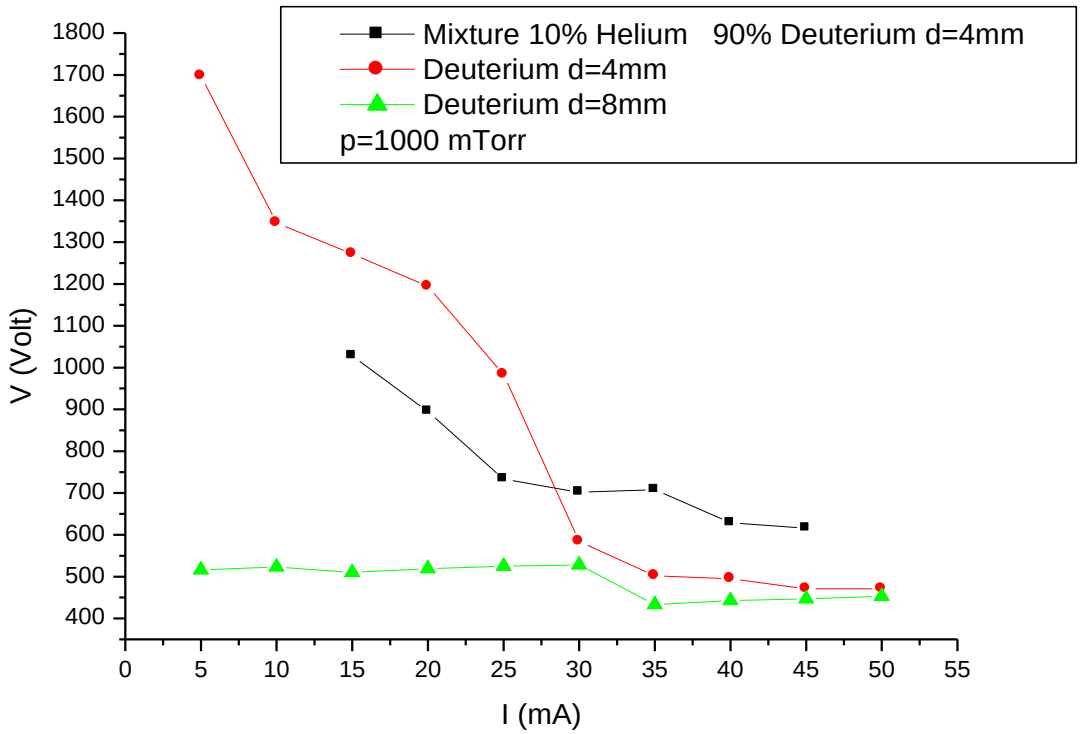

Figure 12: I-V curve for 10% of helium and 90% deuterium at p = 500 mTorr

2.4 The Detector

Several companies have developed specialized silicon p-n junction photodiodes to achieve a good detection efficiency in the soft x-ray photon energy range. In our experiment, we employed a silicon p-n junction photodiode developed by International Radiation Detectors for applications in the soft x-ray (XUV, wavelength range 1800 Å to 2 Å, energy range 7 eV to 6000 eV) spectral region. Unlike common p-n junction diodes, these diodes do not have a doped dead-region and have zero surface recombination resulting in near theoretical quantum efficiencies for XUV photons and other low energy particles. Fig. 13 shows the responsivity of AXUV photodiodes to photons with 10 to 4000 eV energy and to electrons and hydrogen ions with 100 to 40,000 eV energy.

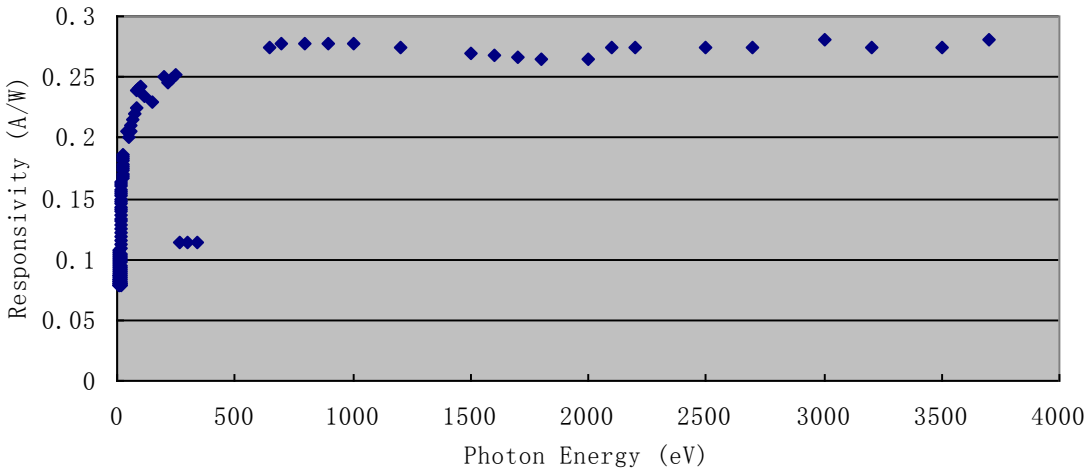

Figure 13: Responsivity of the AXUV photodiodes to photons 100.

The second unique property of the AXUV diodes is their extremely thin (3 to 7 nm), radiation-hard silicon dioxide protective entrance window. Owing to these two outstanding properties, the quantum efficiency (electrons/photon) of AXUV diodes approaches the ideal quantum limit so it can be approximately predicted in most of the XUV region by the theoretical expression. $\eta_{Q=} E_{ph}/3.7$. Here E_{ph} is the photon energy in electron-volts. The only significant quantum efficiency loss is due to the front silicon dioxide window at wavelengths where its absorption and reflection are not negligible (mainly for 7 to 100eV photons). Figure 14 shows the typical quantum efficiency plot of AXUV photodiodes.

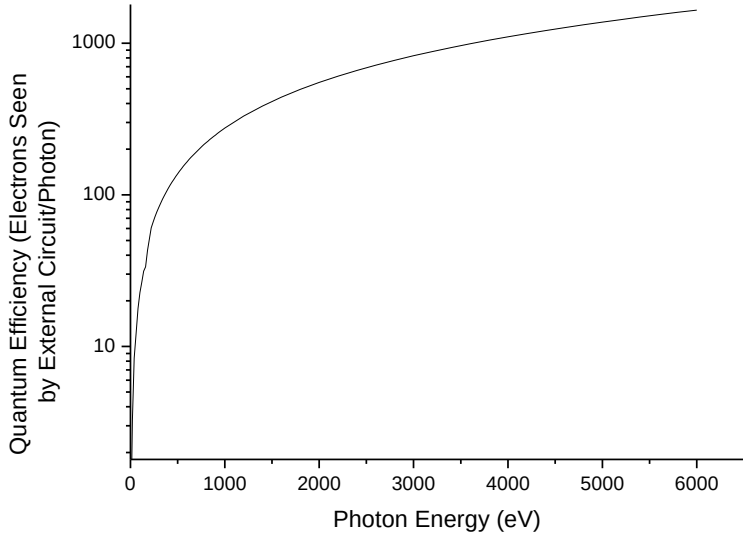

Figure 14: Quantum efficiency of the AXUV 100.

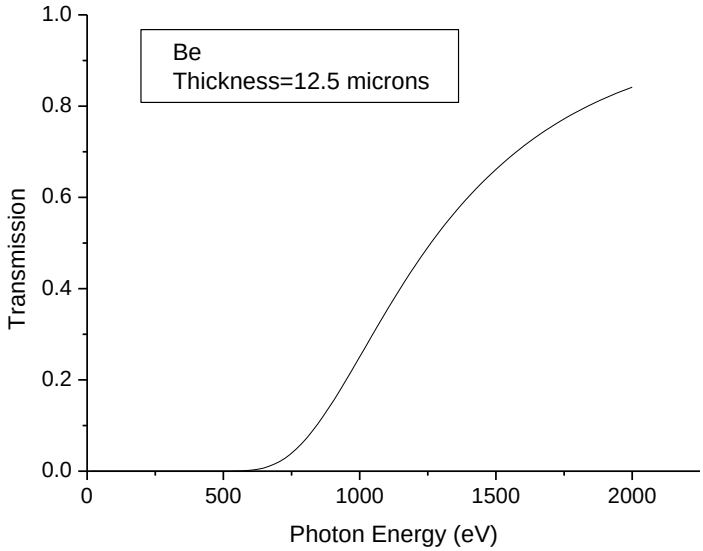

Figure 15: Filter transmission rate as a function of photon energy.

To filter out visible light, and to provide a preliminary indication of the photon energy a beryllium window, produced by MOXTEK (which provides mounted and unmounted beryllium windows for a number of common detector sizes), is added in front of the diode detector. The thickness of our beryllium window is 12.5 µm, and its diameter is 12 mm. Figure 15 shows the transmission rate of the beryllium window as a function of the photon energy. A photograph of the window and detector setup is shown in Fig. 16.

Figure 16: The detector and the beryllium window.

A 0.5mm-thick copper foil was placed in front of the detector for reference background noise measurements. With the current setup, the noise level turned out to be quite low, approx. 0.05 V.

3. Anomalous X-Ray Emission

Following the configuration and gas mixture studies described earlier, the p-n junction detector and Be filter were used in a series of x-ray measurements. Results are described next.

3.1. X-Ray Emission Measurements

We present in this section some representative experimental results illustrating the intense emission of anomalous x-rays observed during certain discharge experiments. The x-ray emission intensity is based on a comparison of the detector signal observed with the Be filter in place versus the signal with the

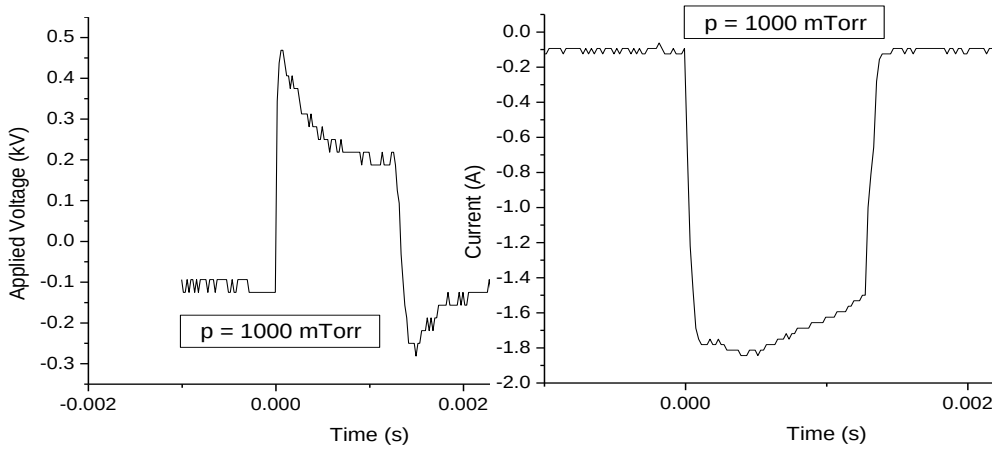

detector totally blocked by the copper foil described earlier.

(a) Voltage **(b) Current (inverted by scope)**

Figure 17: Typical voltage-current pulse characteristics.

Figure 17 (a) shows the pulse voltage shape and (b) shows the current shape. They approximate square waves with peaks of about 250 V and 1.5 amps (about 375 W for 1 msec). The overshoot at the end of the pulses in Fig. 17(a) is due to the lag from the high voltage probe. In reality, the applied voltage is always positive. The corresponding detector response with the detector blocked, Fig. 18, shows a low background signal of about 0.06 V.

Typical unblocked detector signals (but with the Be filter in place) at p = 500 mTorr are given in Figs. 19 (a-c). Clearly strong spikes occur toward the end of the pulse, which do not occur in the background blocked signal. The time width of these spikes varies somewhat from the shorter ones in Figs 19. (a-b) to the wider types occasionally observed as shown in Fig. 19(c). 500 mTorr is near the optimum pressure

for this emission. For example, as the pressure is increased to 1 Torr, the x-ray signal completely disappears as seen in Fig. 18.

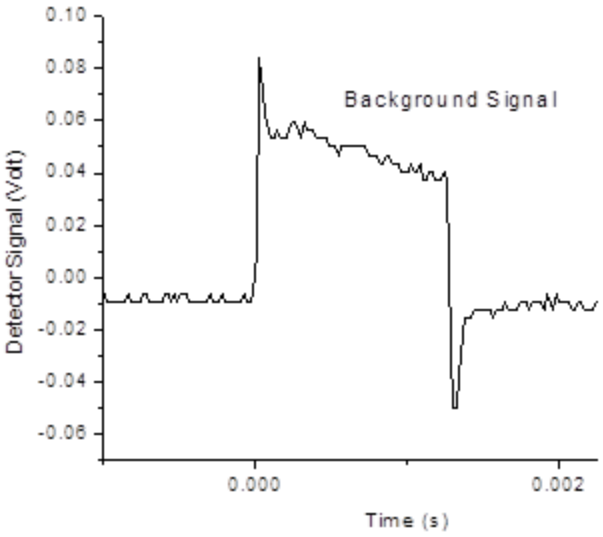

Figure 18: Background signal with detector blocked with copper foil. A background level of ~0.06 V occurs at the start of the pulse and slowly falls to ~0.04V.

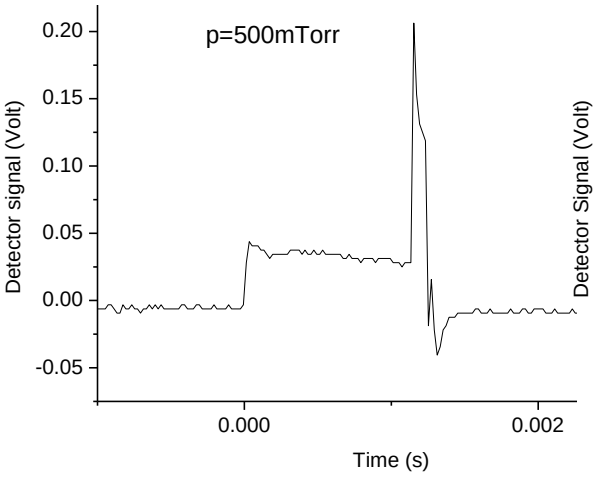

(a)

Detector signal at 500 mT shows strong x-ray emission at the "tail" of pulse. The leading position of the signal (~0.06V) represents the background level corresponding to Fig. 18.

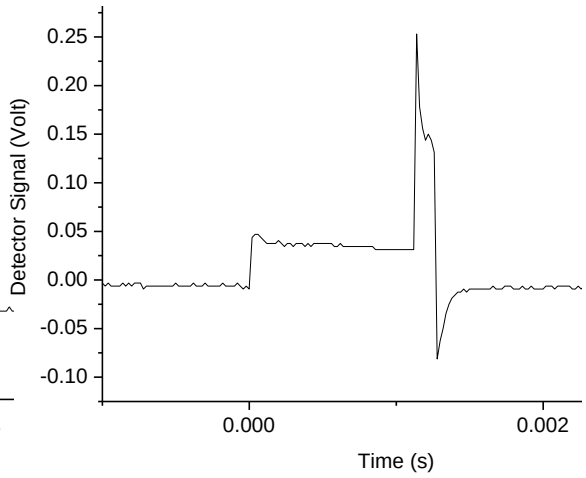

(b)

Duplicate trace at 500 mT.

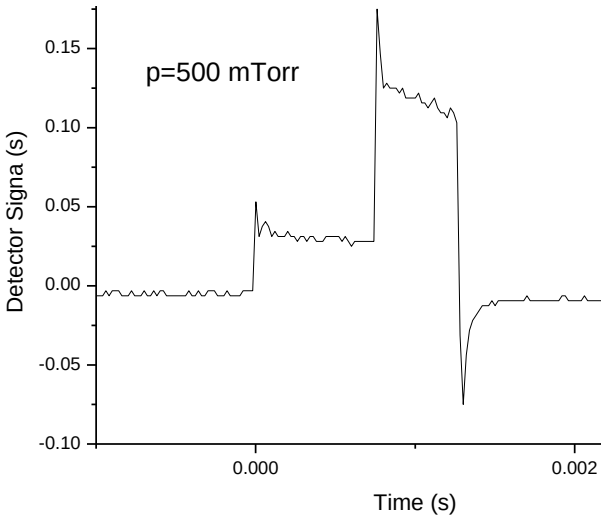

(c)

Another trace at 500 mT showing a broader emission band.

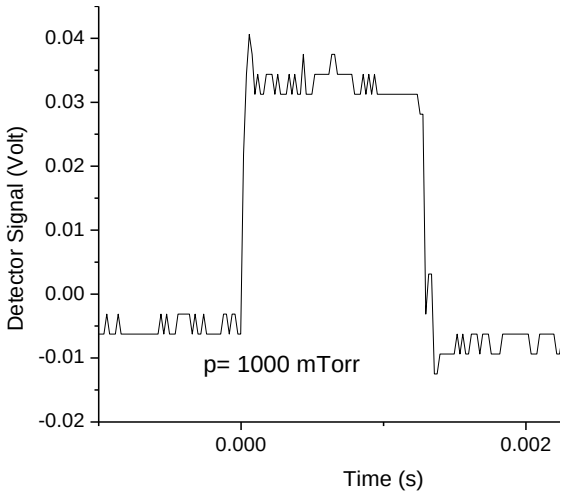

(d)

Detector signal at high presence. At 1000 mT emission stops.

Figure 19: X-ray measurements.

3.2 Data Analysis

From the preceding results, combined with related data obtained in Andrei Lipson's laboratory in Russia, there is very strong evidence for significant soft x-ray yields (> 600 eV) occurring at discharge operating voltages around 300 V. This result is remarkable in that the x-ray energy is higher than the applied voltage – hence the term "anomalous" x-rays. They clearly are generated via a highly nonlinear (multi-excitation step) process. This behavior contrasts sharply with the very small x-ray yields that would be expected from normal charged-particle Bremsstrahlung radiation at these voltages. In addition to the energy difference between the applied voltage and the x-rays, it is important to observe the following:

- The detector (Fig. 1) views the cathode where ion, not electron bombardment, dominates. Thus, again, all evidence is against this being simple electron Bremsstrahlung.

- Bremsstrahlung radiation (x-rays) due to the ion-bombardment of the cathode at these energies is calculated to be negligible, i.e., much smaller than even the 0.05V background signal. Thus the emission process is much more involved. It is thought to be associated with ion cluster effects.

These results are essentially in agreement with Karabut's subthreshold x-ray measurements, giving confidence that further work should enable us to get into a regime of strong coherent x-ray emission. The characteristics of the x-ray quanta generated in the Glow Discharge (GD) bombardment mode can be summarized as follows:

1. The unique peculiarity of this GD is the intense emission of x-ray (1013-1014 1.4 keV x-ray quanta/s-cm2 cathode (Ni, Pd) - cathode at I = 100 -200 mA and V = 0.2 -2.0 kV). This emission cannot be explained by direct ion-electron Bremsstrahlung. In the case of a standard x-ray tube, the x-rays originate from secondary electrons bombarding and slowing down in the anode. In contrast, the contribution of electron Bremsstrahlung radiation in the present GD experiment cannot be significant, because the energy of electrons is too small and the detector does not view the anode surface where they would originate. In the present case the detector views the cathode which is bombarded by ions. The main fraction of the deuteron energy during interactions in the cathode is spent on nuclear recoil (90%). Less than 10% will be transferred to interactions with electrons at near-the-surface of the cathode [4, 5] layer (which has a thickness equal to the deuteron stopping range R < 15 nm [6]) where x-rays could be generated and escape. To further illustrate this point, let us roughly estimate possible x-

ray flux produced by secondary electron braking at the anode using slightly modified formula that is usually applied for calculation of x-ray intensity in x-ray tubes [7]:

$$\Phi_x \sim \alpha K(Z_A J_e \langle U_{GD} \rangle) \quad (1)$$

Where $\alpha \sim 0.1$ is the fraction of deuteron energy spent to induce electron emission; $K = 9.12 \times 10^{-7}$ is the efficiency of x-ray production in x-ray tube from electron braking; $Z_A = 42$ is the atomic number of a Mo anode; $J_e = 100$mA and $\langle U_{GD} \rangle = 1.8$ kV are the discharge current and mean voltage, respectively. For a conservative estimate, we take the electron current and energy to be roughly equal to deuteron parameters.

Substitution of these parameters into Eq. (1) gives us a Bremsstrahlung yield of $\Phi x \sim 10^{12}$ 1.2 keV-quanta/s. This level is about 1-2 orders of magnitude less than the x-ray yield observed in fig. 7 in the present experiment, operating at a similar current and voltage. This is in agreement with the studies by Karabut where the main contribution to the x-ray emission originates from the cathode (Fig. 20). Notice that in this photo the x-ray image diameter coincides with the size of cathode, further localizing its origin.

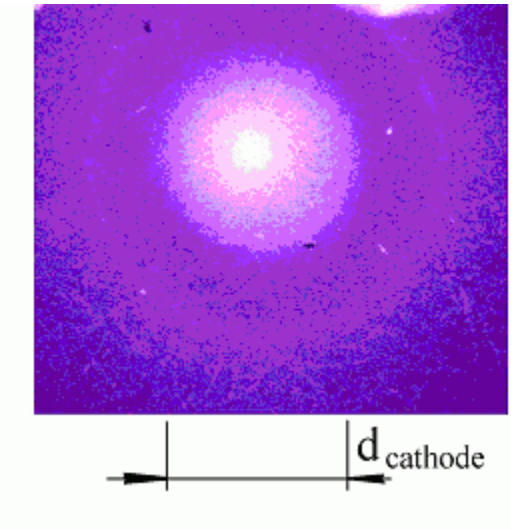

Figure 20: Image of x-ray emission from the cathode using the pinhole camera. The objective is narrowed by use of a 15μm Be shield in front of the camera, showing a bright center spot. Conditions of discharge – J = 150mA, U = 1250 V, p = 5.3 mm Hg, the exposure time – 1000 s. The spot diameter is equal to the cathode size [3].

2. Further proof of anomalous x-ray emission in the GD is given by comparison of the yield and energy of x-ray quanta generated from the Ti-cathode with those parameters of x-ray Bremsstrahlung originating from the deuteron bombardment (ion Bremsstrahlung) of the same cathode. We note that Bremsstrahlung radiation induced by ion bombardment with conventional accelerators in the energy range of E_d < 100 keV is negligibly small and never reported in the literature. Indeed MeV energies are necessary for proton Bremsstrahlung to be used as an instrument in crystalline structure studies [5].

In the present GD experiments it is found that the intensity of X–ray production strongly (exponentially) depends upon the discharge electric power. This is consistent with the assumption that it is driven by deuterium diffusion near the cathode surface.

The observed x-ray dose in this experiment (in Gy, obtained with Thermo luminescent detectors [3]) at constant deuterium pressures is found to be in good agreement with a law:

$$I_x = I_0 \exp[(\varepsilon/kT_m)P^*_x/P^*_0] \qquad (2)$$

where I_0 is the x-ray dose: I_0 = 0.98 Gy for p = 6.0 mm Hg and I_0 = 0.725 Gy for p = 4.2 mm Hg. This eq. (2) assumes deuterium diffusion to escape from the cathode surface with activation energy ε = 0.04 eV [7]; T_m = 1941 K (Ti melting point) and threshold power $P^*_0 \cong$ 6.0 W for both pressures. The graph of P* functions at two constant deuterium pressures is shown in Fig. 21.

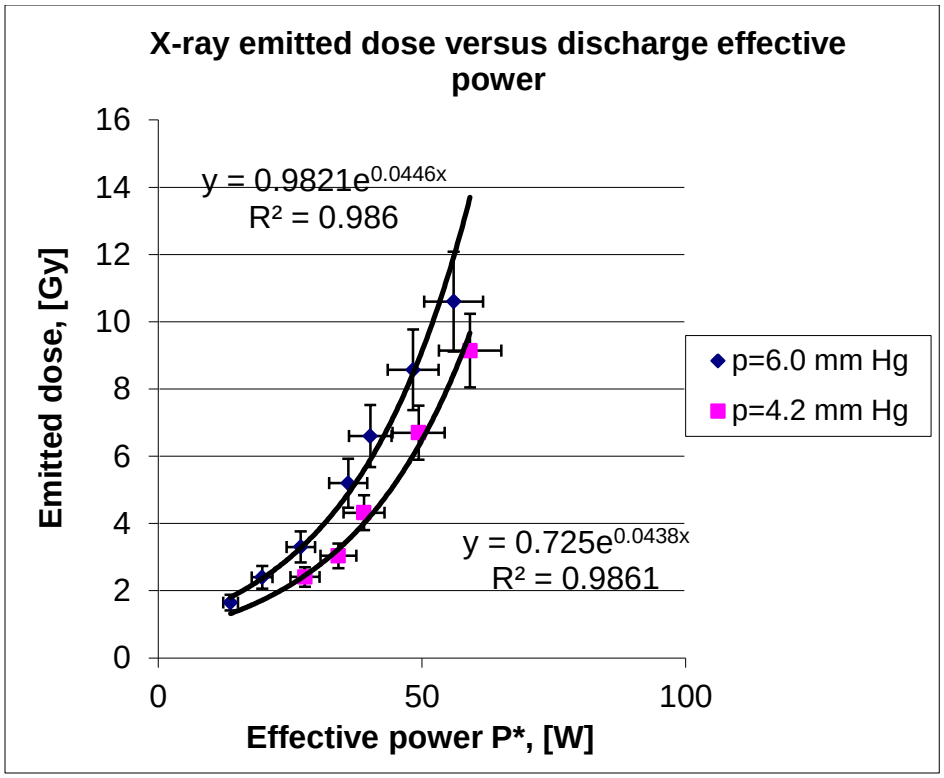

Figure 21: X-ray dose versus GD effective power P* = UIQ.

We can assume that bombarding deuterons generate both secondary electrons (that produce characteristic x-rays) as well as soft Bremsstrahlung radiation during the energy loss in the Ti cathode material. In considering secondary electron Bremsstrahlung radiation, we immediately note that the energy of characteristic x-rays from the Ti cathode would be E_x =460 eV when the energy of bombarding deuteron ranges from 1 to 2 keV. This value is significantly lower than was detected during GD operation (1.4 keV). Indeed, the K_α energy of the Ti-atom is about 4.96 keV and cannot be excited by 1-2 keV secondary electrons. Furthermore, the maximal characteristic energy that could be excited corresponds to the LII shell with energy 460 eV. That value is well below the detection limit. Thus we can neglect characteristic contribution to possible secondary x-ray generation induced by T-cathode deuteron bombardment.

A conservative analysis of Bremsstrahlung radiation directly induced by deuterons, using equations similar to Eq. (1), shows a linear dependences of x-ray quanta energy and intensity of the discharge effective power: P* = UIQ, where U and I are the deuteron voltage and current, respectively and Q = 0.15 is the pulse on-to-off ratio for present pulsed glow discharge. Moreover, the intensity and energy of such a hypothetical Bremsstrahlung is much lower than that detected during glow discharge operation. Notice that maximal x-ray Bremsstrahlung intensity corresponds to quanta with the energy E_x

= 2/3 E_{max} [7], where E_{max} is taken as E_{max} = eU (e is the electron charge and U is the discharge voltage, e.g. equal to the deuteron energy in laboratory system).

These arguments are summarized in Fig. 22, which compares the efficiency of x-ray production per deuteron (representing the number of emitted x-ray quanta as a function of discharge current) versus effective power and in Fig. 23, which compares the x-ray quanta energy versus discharge voltage. The experimentally measured parameters and those calculated accordingly to the conservative estimate of deuteron induced Bremsstrahlung radiation, accordingly Eq. (1) show a dramatic difference.

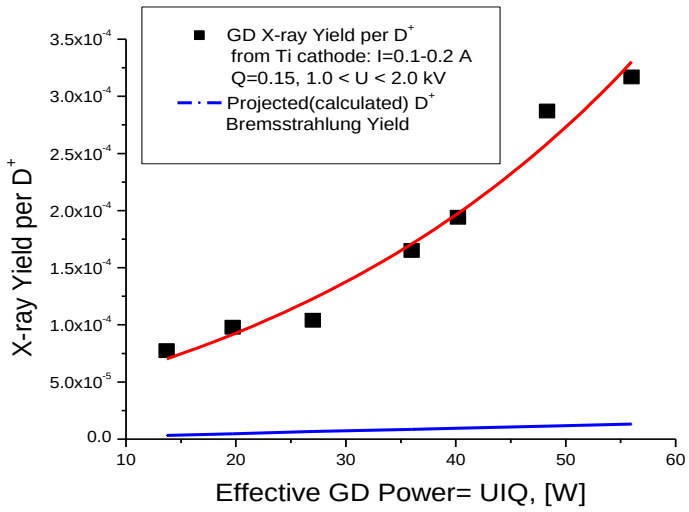

Figure 22: X-ray yield per deuteron in glow discharge versus effective discharge power: points are the experimental yield. The blue curve is the x-ray yield calculated, in assumption of ion induced Bremsstrahlung.

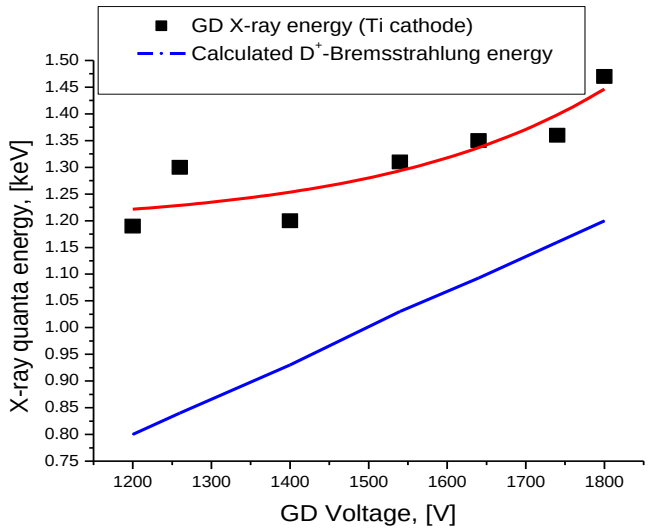

Figure 23: Mean x-ray energy versus glow discharge voltage. Points are the measured energy. The blue curve is the x-ray energy estimated, in assumption of ion induced Bremsstrahlung.

In conclusion, the soft x-ray emission generated from the cathode in the high current glow discharge experiment with voltages ranging from 0.2 to 2 kV cannot be ascribed to either electron or induced x-ray Bremsstrahlung.

4. Theoretical Study of the Emission Process

A possible mechanism to explain the anomalous emissions is the coherent generation of soft x-ray quanta. This is induced by a simultaneous coherent D-diffusion process near the cathode's surface (generating high-order harmonics) and high current deuteron bombardment. These processes result in penetration of recoil deuterons into the inner (LII) electron shell of the cathode material (Ti).

This model suggests penetration of the recoiling deuteron's wave function in the inner shell of the host-metal (Pd, Ti, Ni), excitation of an electron in the inner M(L)-shell, and loss of this excitation energy when the electron returns back to its native orbital [8, 9]. The whole process of "spontaneous" x-ray emission induced by recoiling deuterons during D+- Pd cathode bombardment can be represented as follows:

$$D^+(E_d) + [D_0 + Pd]_{sd} \rightarrow [D_r^+ + Pd(MII)]^* + D_0 \rightarrow DD(U_{MII}) + X(E_d);$$

$$E_d \sim 2.0 \text{ keV}; E(D_0) = kT;$$

$$E(D_r^+) = E_d - kT; E(PdMII) = 600 \text{ eV}, E(X) \sim E_d ;$$

where E_d is the deuteron mean energy in a laboratory system in glow discharge; $[D_0 + Pd]_{sd}$ is the hybridized state of a diffusing deuteron (D_0) s-orbital and d-valence orbital of Pd atom; D_r^+ is the recoiled deuteron produced during projectile deuteron $D^+(E_d)$ interaction with deuterons diffusing near the Pd atom (this interaction should be considered as a quantum coherent process, when a projectile deuteron interacts with the PdDx lattice as a whole); $DD(U_{MII})$ is deuteron screening with participation of inner MII electron shell of Pd atom (here U_{MII} is the screening potential that is equal to energy of this inner shell); X(Ed) is the resulting x-ray quanta with mean energy comparable with that of the projectile deuteron.

The resulting model suggests simultaneous screening of deuteron pairs and induced x-ray emission (short ranged in a time scale, comparable with the time of electron transition in the MII-shell). The screening of deuterons is caused by a large enhancement of DD-reactions observed in glow discharge. The x-ray emission predicted by this model is non-coherent in general, if taken over the whole cathode area. However, coherent nano-sites within the cathode surface area are also expected. The contribution of these sites can be increased dramatically due to special conditions occurring in the glow discharge. These effects cause the deuterium diffusion rate through the whole surface of the metal target to be very high. This condition suggests a very high current density ($I > 100$ mA/cm^2), producing high order

harmonic generation near the cathode surface. Thus, “spontaneous” emission theoretically could be coherent under the super-high current density obtained in the glow discharge. We briefly formulate and roughly estimate such glow discharge conditions for a Ti cathode which is bombarded by a high current, pulsed periodic deuteron beam at I = 200 mA and U ~2.0 kV, as follows:

- At high surface temperature near melting point, e.g. at T = 1940 K, the average deuteron energy near the surface (over its stopping range R_S ~15 nm) E_d = 0.17 eV, and deuteron velocity is $v_d = 4x10^5$ cm/s.
- Under the D-bombardment the main fraction of deuterium flux move inside the cathode toward its surface across of the deuteron stopping range layer: $\Phi_d = 1/3 n_d v_d \sim 10^{29}$ cm^{-2}-s^{-1}, where $n_d \sim 2x10^{23}$ cm^{-3} is the deuterium concentration over the stopping range [10, 11]
- D-diffusion is a coherent process [12] similar to excitation of x-ray lasing in gases by a powerful femtosecond IR laser beam [13, 14]. This IR laser irradiation induces high-order harmonic generation, resulting in lasing in inner electron shells of atom-host [15].
- In the case of glow discharge the deuteron flux effective power density at the active sites (dislocation cores) over the Ti surface would be $P_{off} \approx 10^{14}$ W/cm^2 [3].
- Feasible energy of x-ray laser quanta would be $h\nu = U_e + 3.2\ W_p$ ~1.4 keV, where U_e= 462 eV is the ionization potential of the inner shell (TiL_{II}); W_p = 250 eV is the ponderomotive potential [16] induced by interaction between a coherently moving deuterium flux and bombarding deuterons at P_{off} ~10^{14} W/cm^2.
- D^+ penetration into L_{II} Ti- shell provides a strong electric field suppressing induced x-ray beam de-phasing effects [14].
- Expected duration of x-ray pulses from the Ti-cathode: $t = R_s/v_d$ ~$4x10^{-12}$ s.

The resulting model suggests coherent keV-x-ray quanta generation in the pulsed periodic deuterium glow discharge. It predicts that an increase in the current and voltage of the discharge (I ~10 A and V > 20 keV) could produce the emission of kV energy coherent x-rays.

5. Conclusion

Experiments confirm significant anomalous (collective effect) x-ray emission during discharge operation. Insignificant x-ray yields would be expected due to classical Bremsstrahlung.

- Detector views the cathode where ion, not electron bombardment dominates.
- Ion bombardment induced Bremsstrahlung (x-rays) yields at these energies are virtually negligible.

Yet, quite significant (> 10 mW/ cm2) x-ray yields are observed.

Most striking: > 600 eV x-rays obtained with only a 300 V discharge. This cannot be explained by a classical mechanism such as Bremsstrahlung, suggesting a nonlinear collective phenomenon.

References

[1] A. Karabut, “Research into powerful solid x-ray laser with excitation of high current glow discharge ions,” in *Proceedings of the Eleventh International Conference on Emerging Nuclear Energy Systems*, 2002, Albuquerque, NM, pp. 374-382.

[2]. G. H. Miley, A. G. Lipson, and A. B. Karabut, “A New Type of phonon-driven x-Ray laser,” in Sixth International Committee for future Accelerators, Novel Accelerators and Laser-Beam Interactions, Oxford, England, July 2003.

[3] A. G. Lipson, A. S. Roussetski, A. B. Karabut, and G. H. Miley “Strong Enhancement of DD-reaction and Soft X-ray Generation in a High-current Deuterium Glow Discharge at Voltages 0.8-2.5 keV,” *Journal of Experimental and Theoretical Physics*, vol. 100, no. 6, pp. 1175-1187, June 2005.

[4] D. Pines, *Elementary Excitations in Solids*, New York, USA: J. Wiley, 1963.

[5] A. Benninghoven, F. G. Rudenar, and H. W. Werner, *Secondary Ion Mass Spectrometry: Basic Concepts*, New York, USA: J. Wiley, 1987.

[6] H. H. Anderson and J. F. Ziegle, *Hydrogen Stopping Powers and Ranges in All Elements*, New York, USA: Pergamon, 1977.

[7] D. T. Graham and P. Cloke, *Principles of Radiological Physics*, 4th ed. Edinburgh, UK: Churchill Livingstone, 2003.

[8] P. B. Corkum, “Plasma perspective on strong field multiphoton ionization,” *Physics Review Letters*, vol. 71, no. 13, pp. 1994-1997, 1993.

[9] M. Drescher, M. Hentschei, R. Klenberger et al., “Time-resolved atomic inner-shell spectroscopy,” *Nature*, vol. 419, pp. 803-807, Oct. 2002.

[10] H. Yuki, J. Kasagi, A. G. Lipson, T. Ohtsuki, T. Baba, T. Noda, B. F. Lyakhov, and N. Asami, “Anomalous enhancement of DD Reaction in Pd and Au/Pd/PdO heterostructure targets under low-energy deuteron bombardment,” *Journal of Experimental and Theoretical Physics*, vol. 68, pp. 823-829, 1998

[11] J. Kasagi, H. Yuki, T. Baba, T. Noda, and A.G. Lipson, “Strongly enhanced DD-fusion reaction in metals observed for keV D+ bombardment,” *Journal of the Physical Society of Japan*, vol. 71, no. 12 p. 2881, 2002.

[12] Y. Fukai and H. Sugimoto, “Hydrogen diffusion in metals,” *Advances in Physics*, vol. 34, no. 2 pp. 263-326, 1985.

[13] H. Daido, “Review of soft x-ray laser researches and developments,” *Reports on Progress in Physics*, vol. 65, pp. 1513-1576, 2002.

[14] J. Seres, E. Seres, A. J. Verhoef et al., “Source of coherent kiloelectronvolt x-rays,” *Nature*, vol. 433, p. 596, Feb. 2005.

[15] E. A. Gibson, A. Paul, N. Wagner, et al., “Coherent soft x-ray generation in the water window with quasi-phase matching,” *Science*, vol. 302, p. 95, 2003.

[16] R. R Freeman, P. H. Bucksbaum, T. J. McIlrath, “The ponderomotive potential of high intensity light and its role in the multiphoton ionization of atoms,” *IEEE Journal of Quantum Electronics*, vol. 24, p. 1461, 1988.